Electrochemistry at High Specific-Area Carbon Electrodes: Applications to Adsorptive Purification of Waters and to Charge-Storage by Supercapacitors

KUI 10/2005
Received August 16, 2004
Accepted January 11, 2005

B. E. Conway, J. Niu and W. G. Pell*

Chemistry Department, University of Ottawa,
10 Marie Curie Street, Ottawa, ON. K1N 6N5, Canada

Several forms of the element, carbon (C), are utilized in major ways in electrochemistry as high specific-area powders, felts, woven cloth, aerogels or "fullerene" tubes. The present paper reviews and reports recent works using high specific area (~ 2500 $m^2 g^{-1}$) C-cloth as an electrode material for adsorptive collection of organics from model waste-water solutions and for electric charge storage and delivery by electrochemical capacitors (so-called Supercapacitors). Both these aspects of high-area C-electrode behaviour arise from properties of the interphasial double-layer at which electrosorption and charge accommodation can take place, with the latter observably influencing the former.

For simple aromatic heterocyclic compounds, such C-material exhibits high effectiveness for adsorptive collective removal and, importantly, major changes of extents of adsorption with applied potential or current, and with change of solvent type.

Complementarily, the same high specific area C-cloth electrodes exhibit large capacitance density (250 ~ 500 F g^{-1}) enabling them to be used as Supercapacitor electrodes. Examples are shown of characterization of charge storage and delivery at such electrodes, especially at high rates, providing attractive values of power-, and energy-density, the former being much higher than with batteries.

Keywords: *Carbon-cloth electrode, electrochemical capacitor, supercapacitor, waste-water purification, adsorption, electrosorption*

Introduction

High specific-area carbon materials, having areas on the order of 1000 $m^2 g^{-1}$, or greater, are finding major applications as electrodes for electrochemical waste-water purification[1–4] and for electrical charge and energy storage and delivery in so-called Supercapacitors.[5,6] Apart from high-area C powders produced by thermal carbonization of wood or coconut shells, a variety of new materials is now available arising from carbonization of organic polymers, e.g. polyacrylonitrile, polyphenylene oxides, cellulose, etc, and as C aerogels and C nanotubes (fullerenes). Carbon materials, thus generated, can be produced in the form of C paper and cloths woven from high specific-area C fibres that are specially suitable for fabrication of electrodes having good mechanical integrity, in contrast to C powders that require binders. Preparation of very high specific-area C materials (≥ 1000 $m^2 g^{-1}$) requires special (usually proprietary) techniques of further conditioning, e.g. at high temperatures in steam or N_2, enabling nano-scale pores and high surface area to be opened up. Such treatments give rise to material-specific pore-size distributions that determine properties such as double-layer capacitance and density of surface-group functionalities,[8] e.g. COOH, C–OH, C = O, lactone and quinonoid structures that importantly determine the surface-chemical properties of the C materials and, for supercapacitors, the extents of redox pseudocapacitance.[9,10,11]

The use of high specific-area C powder, felt or particle materials for solution purification goes back to classical organic chemistry where such materials are employed in final work-up of preparations for pure product separation. Such procedures have given rise, in recent years, to attempts to utilize high specific-area C materials on a larger scale[1] for beneficiation of industrial waste waters by adsorption and / or by electro-oxidation or electro-reduction of impurities in water solutions.[1,2] This has now become a substantial electrochemical engineering application as well as a stimulant for more fundamental understanding of electro-sorption and electrode processes in porous electrode materials, including processes involved in chromatography. Seminal works in the former areas were those by *de Levie*[12] and by *Keiser* and *Beccu*.[13]

* e-mail via: wpell@science.uottawa.ca
Fax: 613-562-5170

In a different but related direction is the area of high specific-area C materials used as media in which electrical charge can be stored and delivered non-Faradaically[14,15] through the *double-layer capacitance*[15] at such materials. This is to be contrasted with charge storage indirectly in batteries where Faradaic charge-transfer processes are involved, coupled directly with chemical changes associated with redox reactions. These aspects are treated in the section of this paper on Electrochemical Double-Layer Capacitors.

The above two, seemingly different aspects of the use of high specific area electrodes that are treated in the present paper actually have a close fundamental relationship: that is, the role of high distributed surface area at which electrosorption of organics or ions takes place in the double-layer or at which (Supercapacitor case) electric charge separation (ions and electrons) arises across the electrode's interface giving rise to accumulation or delivery of large charge capacities, on the order of 300 C g^{-1}. In the case of adsorption of organics in water beneficiation, the double-layer capacitance is usually lowered, as it is at the mercury electrode.[15,16] These two complementary aspects of carbon electrode behaviour will be reviewed and treated in the following two sections of the present paper. Recent work[1,4,17,18] has involved generation of a large volume of results, so only selected examples can be reviewed here, arising substantially from our newest research activities in the two fields.

Adsorption and electrosorption of organics at high, specific-area carbon-cloth electrodes

Methodology of adsorption studies by means of *in situ* UV spectrophotometry

Environmentally unfriendly contaminants of water are often present at biologically significant but very low concentrations. Accordingly, in the present studies at C, adsorption extraction of organics has been modeled in solutions of *e.g.* xanthine, pyridine, 1,4-pyrazine (the para, di-*N* analogue of pyridine which has no net dipole moment, contrast pyridine) and aniline. By means of the UV spectrometric technique, adsorptive extraction from aqueous solution can be studied directly in quite dilute solutions ($10^{-4} \sim 10^{-5}$ mol dm^{-3}) owing to the high extinction coefficients of these model adsorbed "impurities" in the UV. Other molecules or inorganic ions that have colour in the visible can also be studied, or coloured coordination complexes can be generated.

Studies of adsorption of several organics, such as pyridine, 1,4-pyrazine and aniline, that have electronically conjugated structures were made by *in situ* UV spectrophotometry over the spectral range of ca. 200 – 290 nm, using a V-shaped cell sealed to a quartz optical cuvette, designed to provide also the opportunity for electrochemical polarization (positive or negative directions) of the woven C-fibre electrode. The choice of model organic adsorbates was dictated by two factors: their strong extinction coefficients in the UV and their potentiality for ionization by protonation in acidic media so that comparisons could be made between their electro-sorption behaviours as cations or as neutral, uncharged molecules. The UV absorption experiments were conducted by means of a computer-controlled Cary 1E type UV/VIS spectrometer. Electrical polarization of the C electrodes was made galvanostatically at various currents in positive or negative directions, or potentiostatically using regular electrochemical instrumentation. An important aspect of this procedure of polarization, hitherto not seemingly employed in water purification techniques using carbon, is that we have discovered large effects of electric polarization that can greatly improve extents, rates and efficiencies of removal of organics from waste-waters.

For each compound studied, Beer's Law calibrations were made in the cell to relate optical absorbance to adsorbate concentration in solution. The quantity of organic solute adsorbed at an electrode surface was calculated by means of Eq. (1), based on the known specific surface area of 2500 m^2 g^{-1} for the C-cloth used:

$$\Gamma = \frac{(c_o - c_t)V}{2.5 \times 10^7 m} \text{ mol cm}^{-2} \quad (1)$$

where Γ is the adsorbed quantity of the investigated species, directly recorded at a particular surface charge-density during slow galvanostatic polarization (see below), V is the volume, m the mass of the C-cloth module, and c_0 and c_t are the initial concentration and the concentration at time t, during the galvanostatic polarization, respectively. For the particular results obtained in the present work, m was 0.026 g (dry mass of the C).

Carbon-cloth electrode material for study of the adsorption behaviour of pyridine, 1,4-pyrazine and aniline in aqueous solution

The high specific area C electrode material was Spectracarb woven C-cloth having a BET area of ca. 2500 m^2 g^{-1}. This material has good mechanical integrity (contrast C powders) and can be made into mechanically stable electrode configurations. Mass of the C-cloth were recorded prior to samples being formed into electrodes so the double-layer capacitance-density and real areas were known, accurate to 1 – 2 %.

Electrochemical characterization of the C-cloth electrodes was made by means of cyclic voltammetry conducted at various sweep-rates, ν (V s^{-1}), enabling the specific capacitance, C, (F g^{-1}) to be determined as $C = i/\nu$ where i was the recorded current-response as a function of polarization potential and sweep-rate, as illustrated in Fig. 1.

Adsorption behaviours of the organics as a function of time and potential

Fig. 2 shows first the time-dependence of adsorption of pyridine at the C electrode on open-circuit together with the increased rate and extent of adsorption upon application of a negative polarization current of 1 mA. It is seen that polarization has a major effect on the adsorption behaviour, increasing both its rate and the extent of adsorption after sufficient periods of polarization. Fig. 3 shows, for comparison, the pyridinium iom becomes desorbed and the population of the double-layer adjusts as at Hg[15] including the effects due to differences of orientation of water-solvent dipoles.[19]

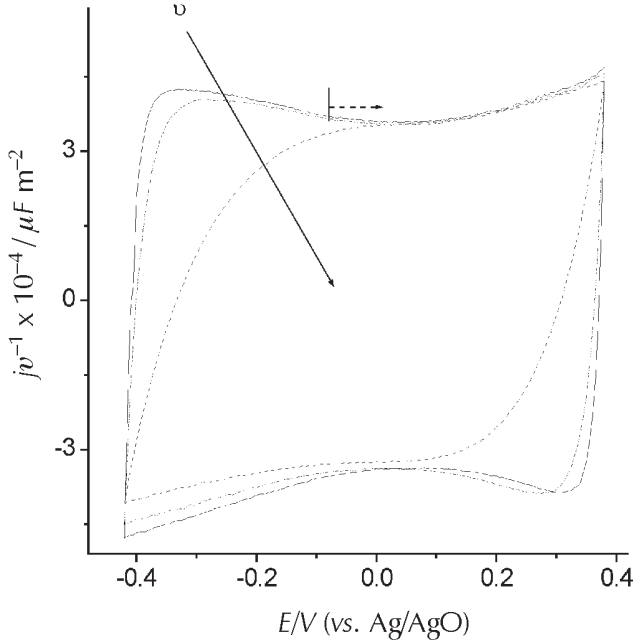

F i g . 1 – *Series of cyclic voltammetry profiles for the porous C electrode recorded at sweep-rates ν = 1, 2, 5, 10 and 25 mV s⁻¹, characterizing the overall differential capacitance, plotted as, C = j/ν. Arrow indicates sequence of increasing sweep-rate. The dashed arrow represents the starting potential and direction of polarization in the adsorption measurements.*

S l i k a 1 – *Serija profila cikličke voltammetrije za porozne C--elektrode zabilježenih pri brzinama promjene napona od 1, 2, 5, 10 i 25 mV/s koji označuju ukupni diferencijalni kapacitet prikazan kao C = j/ν. Strelica pokazuje redoslijed sve bržih promjena napona. Crtkana strelica predstavlja početni potencijal i pravac polarizacije pri mjerenju adsorpcije.*

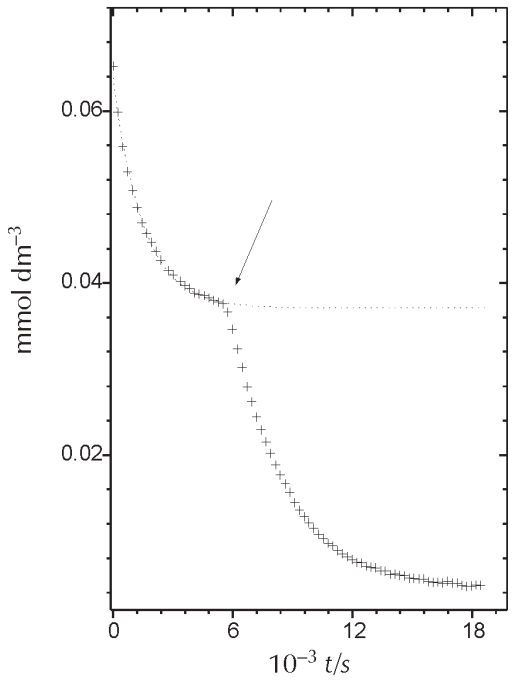

F i g . 2 – *Time-dependence of adsorption of pyridinium ion in aq. H_2SO_4 on open-circuit followed by application of polarization at –1 mA*

S l i k a 2 – *Vremenska ovisnost adsorpcije piridinijevog iona u vodenoj otopini H_2SO_4 pri otvorenom krugu prije polarizacije s –1 mA*

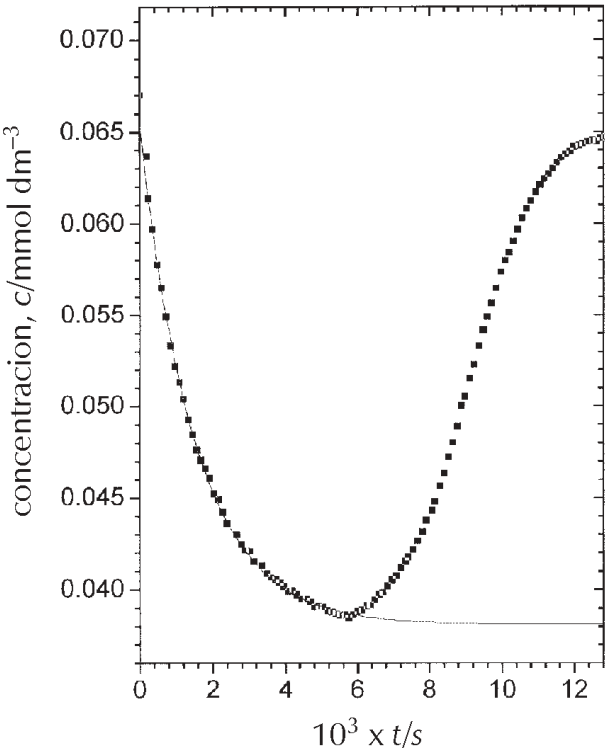

F i g . 3 – *As in Fig. 2 but with application of positive current polarization*

S l i k a 3 – *Kao na slici 2, ali kod polarizacije s pozitivnom strujom*

It is important to note here that adsorption of organics from solution differs qualitatively from that directly from the vapour phase: from solutions, the adsorption process is a *substitutional one* in which previously adsorbed water molecules must become *displaced* from the C surface by incoming organic adsorbate as represented by the quasi-chemical process, written below, for adsorbate A *vs.* solvent S:

$$\text{A (in solution)} + n\ \text{S (at C)} \rightarrow \text{A (at C)} + n\ \text{S (in solution)} \quad (2)$$

where *n* solvent molecules, S, previously adsorbed per cm^2, are displaced by the adsorbate, A, and released into solution; *n* is determined by the ratio of effective molecular areas when S is displaced by A. This process can be potential-dependent, as realized by *Butler,*[16] and depends on the difference of electric polarization of A and S (per unit volume) and of molecular projected areas. Thus, the adsorption of A is competitive with that of S and depends on the difference of Gibbs energies of adsorption of A and S at the C which also affects the *kinetics* of the adsorption (Fig. 2) which are found to be dependent on potential.

The course of the time-dependent adsorptions in Figs. 2 and 3 is found to be first-order but this is probably pseudo-first-order owing to process (2) where S is in excess. Analogous results are found for adsorption of 1,4-pyrazine and aniline where effects of applied electrochemical polarization also arise both at neutral and acidic pH.

Of special interest are pH effects with these "*N*"-functionalized organics which become ionized as $–NH^+$ cations in acidic media. Then, very strong effects of electrode polarization arise for obvious electrostatic reasons in the double-

layer and the organic cations are expelled from the interphase, as shown in Fig. 4, under positive polarization but are strongly adsorbed under application of negative currents. The same effects arise, as may be expected, with the quaternary *N*-Me-pyridinium cation, which has a state of ionization independent of pH.

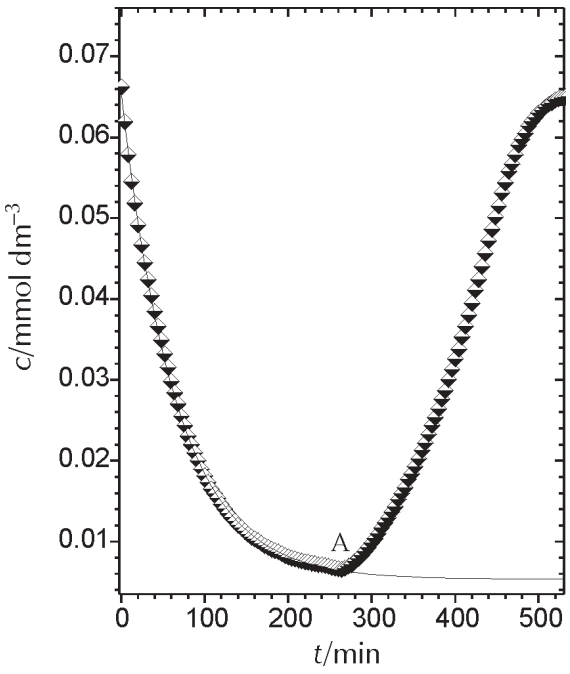

F i g . 4 – *Effects of negative and positive polarization at 1.0 mA on pyridinium ion adsorption in aq. H_2SO_4, indicating complete desorption when positive polarization is applied*

S l i k a 4 – *Utjecaj negativne i pozitivne polarizacije pri 1 mA na adsorpciju piridinijevog iona u vodenoj otopini H_2SO_4; vidi se potpuna desorpcija uz pozitivnu polarizaciju*

With the pyridinium cations, it is of interest that change of direction of polarization leads to quantitatively reversible adsorption/desorption at the C-cloth electrode as illustrated in Fig. 5. The time-scales, however, are relatively slow owing to the requirement for diffusion into, or out of, the porous C matrix. This aspect of reversibility of the adsorption has practical value with ionic contaminants since, following adsorptive collection of such impurities in water under an appropriate direction of polarization, a free electrode surface can be regenerated by opposite polarization with removal of the accumulated adsorbate into another collection reservoir (at higher concentration) in a cyclic regime.

Solvent effects in the adsorption

Process (2) emphasizes the competitive nature of electrosorption of organics from water solutions. In order to evaluate this aspect in more detail, we have compared the adsorptive behaviours of pyridine, 1,4-pyrazine and aniline from acetonitrile, ethanol and *n*-propanol with that from the water solvent (Fig. 6), and the effect of imposed polarization at +1.0 mA. Major solvent effects are observed as illustrated and compared in the series of figures 6a to 6f below. Fig. 7 shows that, *e.g.* adsorption of aniline is much stronger in the aqueous medium than in the other solvents, especially in CH_3CN where it is almost negligible. This

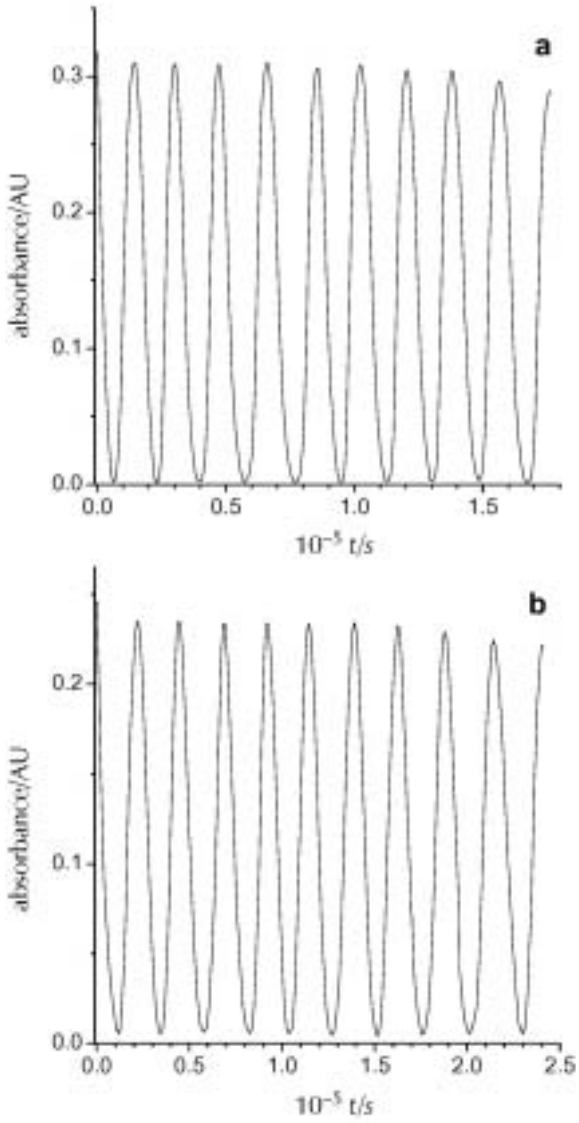

F i g . 5 – *Sequence of positive and negative polarization for (a) N-Me-pyridinium cation and (b) pyridinium cation adsorption at the C electrode showing quantitative reversibility of the adsorption/desorption processes*

S l i k a 5 – *Redoslijed pozitivne i negativne polarizacije za adsorpciju (a) N-Me-piridinijevog kationa i (b) piridinijevog kationa na C-elektrodi, vidi se kvantitativna povratnost procesa adsorpcija/desorpcija*

suggests that the adsorbate/solvent interaction, in bulk solution, is a key factor in selective adsorptive removal of organics from solution. In the practical case of water as solvent, the best adsorptive collection effectiveness is achieved and this can be attributed to *hydrophobic interactions*[22] in process (2) between the organic solutes and the strongly structured and H-bonded water medium. This is also manifested in the surface activity of such organics at the air/water interface as measured by surface-tension changes.

Orientation of adsorbate and solvent molecules at polarized carbon electrodes

At Hg electrodes, measurements of shifts of electrode potential (relative to the potential of zero charge) with increasing concentration of an organic adsorbate, enables the

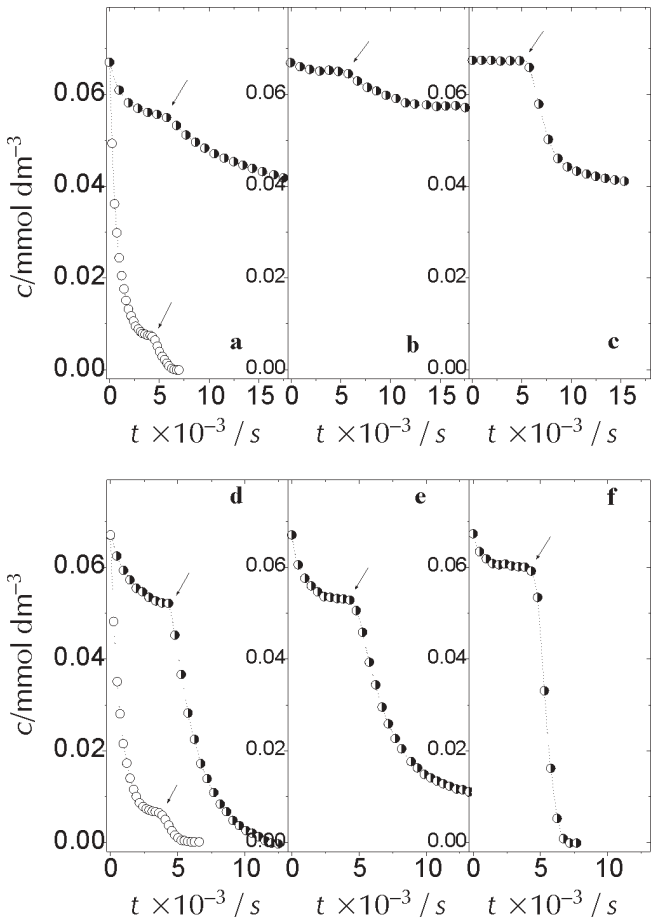

F i g . 6 – *Concentration changes of pyridine (**a, b** and **c**) and aniline (**d, e** and **f**) in EtOH (**a** and **d**), n-propanol (**b** and **e**) and MeCN (**c** and **f**) first by adsorption on open-circuit to achieve a steady state, then starting electrosorption, as indicated by the arrows, at +1.0 mA. Curves in (**a**) and (**d**) represent the corresponding results obtained in H_2O for pyridine and aniline, respectively.*

S l i k a 6 – *Koncentracijske promjene piridina (**a, b** i **c**) i anilina (**d, e** i **f**) u EtOH (**a** i **d**), n-propanolu (**b** i **e**) i MeCN (**c** i **f**), najprije za adsorpciju kod otvorenoga strujnog kruga kako bi se uspostavilo ravnotežno stanje, a zatim početak adsorpcije pri +1 mA, kako pokazuje strelica. Krivulje predstavljaju odgovarajuće rezultate u H_2O dobivene za piridin (**a**) i anilin (**b**).*

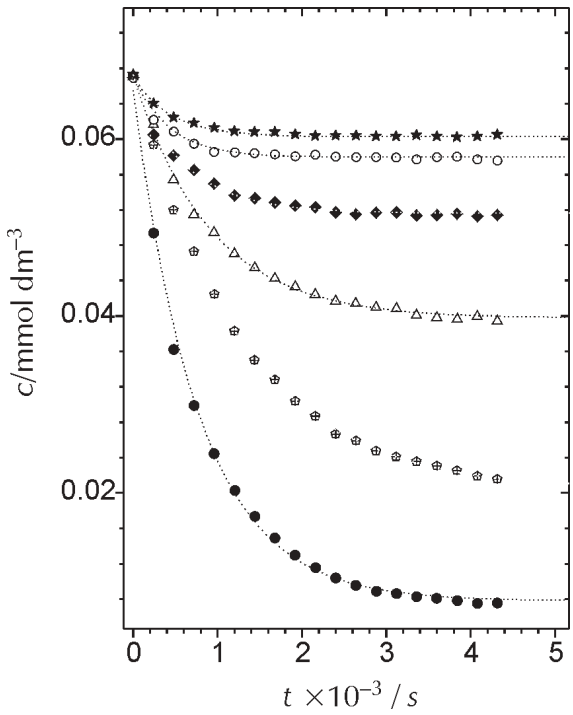

F i g . 7 – *Solvent effect on adsorption of aniline in MeCN + H_2O mixtures on open-circuit: 100 % MeCN (★), 75 % MeCN + 25 % H_2O (○), 50 % MeCN + 50 % H_2O (■), 25 % MeCN + 75 % H_2O (Δ), 5 % MeCN + 95 H_2O (⊗), i 100 % H_2O (•)*

S l i k a 7 – *Utjecaj otapala na adsorpciju anilina u smjesi MeCN i H_2O pri otvorenom krugu; 100 % MeCN (★), 75 % MeCN + 25 % H_2O (○), 50 % MeCN + 50 % H_2O (■), 25 % MeCN + 75 % H_2O (Δ), 5 % MeCN + 95 H_2O (⊗), and 100 % H_2O (•)*

surface potential ($\Delta\chi$) change due to dipole adsorption and solvent molecule orientation to be derived (the so-called Esin and Markov effect). Such experiments can also be conducted at the C-cloth electrode with results shown below for pyridine and the non-dipolar 1,4-pyrazine. Unfortunately, no potential of zero charge can be identified for porous carbons owing to their porous, distributed structure with no unique crystalline surface. However, we have been able to determine values by conducting the Esin and Markov type of experiment by referring potential changes due to adsorption to the potential of a stable reference electrode, here silver/silver oxide.

Charging experiments at various controlled organic adsorbate concentrations not only give information on adsorptive collection of the adsorbate on the high-area C (Figs. 2 to 6) but enable calculations of the orientation of dipolar adsorbates and of solvent-water dipoles to be made in terms of resulting oriented dipole potentials, χ, for various changes, Δq, of surface charge-density, q, giving a molecular picture of the adsorbate/C interphase, in the following way. Since, according to Eq. 2, adsorption of an organic will replace water dipoles already adsorbed from the solvent medium, the surface potential changes due to orientation of the polar organic (here pyridine) are the sum of changes of χ due to solvent displacement and of the χ due to orientation of the adsorbate itself. The change of surface dipole potential, $\Delta\chi_{H_2O}$, corresponding to the component of surface-potential change for solvent (H_2O) replacement by either pyridine or 1,4-pyrazine at surface concentrations Γ, for a given Δq value, will be given, in the simplest analysis, according to the model of Bockris et al.,[19] by:

$$\Delta\chi_{H_2O} = n\Gamma \frac{(N\uparrow - N\downarrow)}{N_T} \cdot \frac{4\pi\mu_{H_2O}}{\varepsilon_s} \qquad (3)$$

where $N\uparrow$ and $N\downarrow$ are the populations of solvent molecules in the BDM model,[19] oriented (limitingly) in "up" ($\uparrow$) or in "down" ($\downarrow$), directions, i.e., normal to the electrode field out of a total, N_T, of water molecules cm^{-2}; μ_{H_2O} is the dipole moment of H_2O in the interfacial water structure, ε_s is the local dielectric constant of water in the inner layer[19] and n (cf. Eq. 2) is the number of the adsorbed water molecules replaced by each organic adsorbate molecule. Strictly, $\Delta\chi_{H_2O}$ will tend to be diminished with increasing solvent-dipole orientation due to mutual depolarization between nearest neighbour dipoles, an effect that will also arise in an oriented array of pyridine dipoles (cf. Eq. (3).

We can write the component of change of surface-dipole potential, $\Delta\chi_{Py}$, associated with orientation of the dipolar pyridine molecule itself as:

$$\Delta\chi_{Py} = \frac{4\pi\mu_{Py}\,\Gamma}{\varepsilon_s} \tag{4}$$

where μ_{Py} is the dipole moment of pyridine and ε_s is an effective dielectric constant of the interphase. This component combines with the change of $\Delta\chi$ due to displacement of the previously oriented solvent H_2O dipoles as given by Eq. (3), thus leading to a net surface-potential change (Esin and Markov effects) of

$$\Delta\chi = \Delta\chi_{H_2O} + \Delta\chi_{Py} = n\Gamma\frac{(N\uparrow - N\downarrow)}{N_T}\cdot\frac{4\pi\mu_{H_2O}}{\varepsilon_s} + \frac{4\pi\mu_{Py}\,\Gamma}{\varepsilon_s} \tag{5}$$

The required extents of adsorption per m² are directly obtained from the *in situ* spectrophotometric data (Eq. 1), and the EM shift, ΔE, experimentally derived, is equal to in Eq. 5.

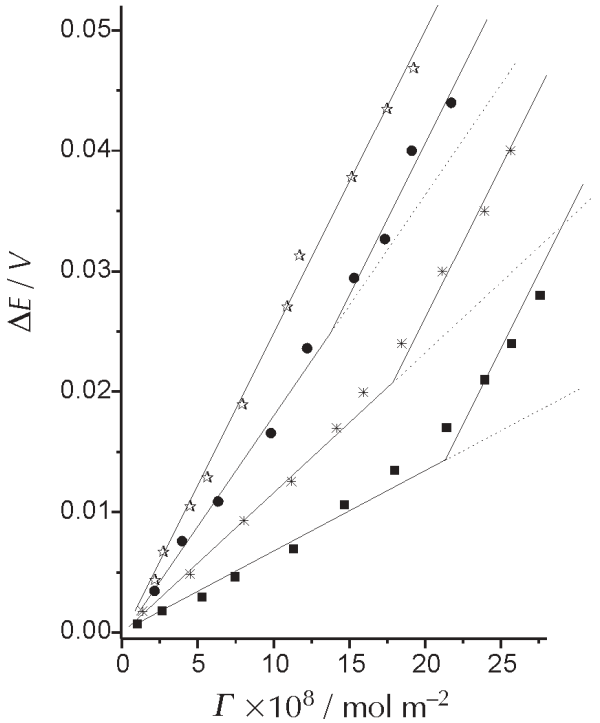

Fig. 8 – *Esin and Markov type plots for effects of pyridine adsorption at the carbon electrode; shifts of potential, ΔE, at four values of change of surface charge Δq (based on data derived relative to the reference potential of –0.08 V, Ag|AgO) plotted vs extents of adsorption of pyridine, Γ: (■) 0.5 ×10⁻⁴ C m⁻²; (✷) 4 10⁻⁴ C m⁻²; (●) 6 × 10⁻⁴ C m⁻² and (☆) 10 10⁻⁴ C m⁻². Dashed lines are extrapolation of the lower-slope regions of the plots beyond the inflection points, towards higher Γ values.*

Slika 8 – *Prikazi tipa Esin i Markov za utjecaj adsorpcije piridina na ugljenoj elektrodi; pomak potencijala, ΔE, kod četiri razine veličine promjene površinskog naboja, Δq, (temeljeno na izvedenim podacima u odnosu na potencijal od –0,08 V prema Ag/AgO), prikazana kao funkcija stupnja adsorpcije piridina Γ: (■) 0.5 ×10⁻⁴ C m⁻²; (✷) 4 10⁻⁴ C m⁻²; (●) 6 × 10⁻⁴ C m⁻² and (☆) 10 10⁻⁴ C m⁻². Crtkaste linije su ekstrapolacija nižeg područja prikaza iza točke infleksije, prema višim vrijednostima Γ.*

It is seen from Fig. 8 that at the C-cloth electrode surface, $-\Delta E$ at first increases as Δq becomes more positive due to solvent replacement in the interphase by pyridine, thus diminishing the solvent orientation contribution to $\Delta\chi$ (Eq. (5)) while the dipolar pyridine itself becomes increasingly oriented leading to an increase $\Delta\chi_{Py}$ (Eq. 4). Here the two effects are considered to be independent though coupling through H-bonding and mutual depolarization between oriented H_2O and pyridine dipoles at less than full coverage by the latter adsorbate could be involved. The *difference of the slopes* of the two regions would give the contribution due to pyridine orientation, taking into account the diminishing solvent orientation component (Eq. 3) with increasing Γ of pyridine at a given Δq. Evidently, pyridine has a strong interaction with the positively charged surface[17] because of its large dipole moment and the unshared electron pair on its N atom. Thus, it is no surprise that the polar pyridine molecules contribute an EM effect, as at Hg, corresponding to the second term of Eq. (5).

Over the regions of Γ values where the orientation transition has taken place (Fig. 8), increasing coverage (Γ) by pyridine (now oriented) will continue to displace previously oriented water molecules with a resultant change of $\Delta\chi_{H_2O}$ in the opposite direction.

Further insight into the situation implied by the two-term equation (5) was obtained by study of the adsorption of the non-dipolar adsorbate, 1,4-pyrazine which has zero dipole moment and hence, itself, will not tend to be oriented in the double-layer field; however, it will displace oriented H_2O dipoles and give an EM shift corresponding to the first term of Eq. (5). Fig. 9 shows clearly that this expectation is borne out and the EM shift is linear in Γ (Eq. 1) without any inflection.

The differences between the slopes of the upper regions of the lines for pyridine (Fig. 8) from those for lower regions, in relation to the slopes of the single-regions of the lines for 1,4-pyrazine (Fig. 9) confirm the basis of interpretation of the results for pyridine that the lower slope regions correspond mainly to displacement of *n* oriented water molecules by pyridine molecules not yet themselves oriented by the interfacial field determined by Δq.

Electrochemical double-layer capacitors (Supercapacitors)

Significance of interfacial capacitance of electrodes

Electrodes, including C, not only provide a polarizable interphase in which adsorption of organic solutes takes place but also an interphase at which positive or negative electron charge densities can be accumulated in response to changes of electrode potential. Thus, electrode interfaces with electrolytes universally exhibit an interfacial capacitance, C_x which arises from the separation of accumulated positive charges (ions in solution) and electrons (at the surfaces of metals or semi-conductors).[15] The effective separation is on the order of 0.2 to 0.3 nm though there is always an associated diffuse distribution of ions into solution, depending on electrolyte concentration, or of electrons and holes in semi-conductor electrodes.

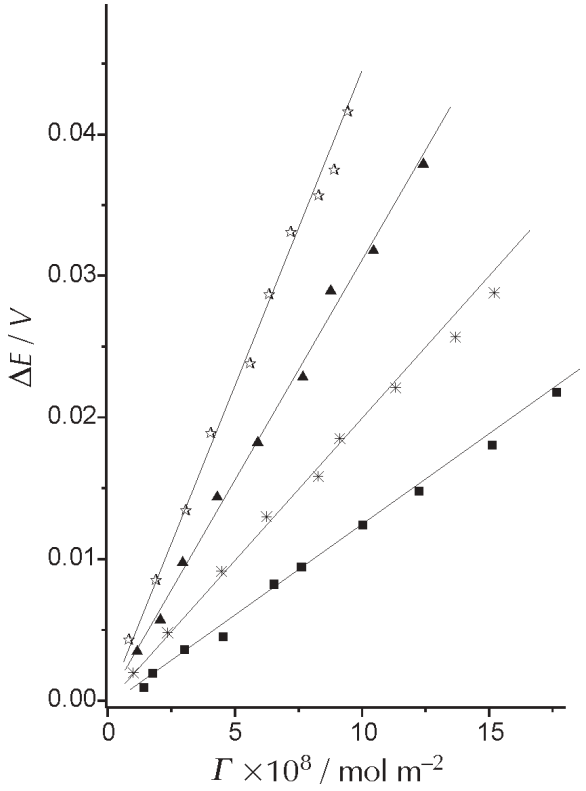

F i g . 9 – *Esin and Markov type plots for effects of 1,4-pyrazine adsorption at the carbon electrode; shifts of potential, ΔE, at four values of change of surface charge Δq (based on data derived relative to the reference potential of –0.08 V, Ag/AgO) plotted vs extents of adsorption of 1,4-pyrazine, Γ: (■) 0.5 10⁻⁴ C m⁻²; (✳) 4 × 10⁻⁴ C m⁻²; (▲) 6 × 10⁻⁴ C m⁻² and (☆) 10 × 10⁻⁴ C m⁻². (Note absence of inflections of the kind observed for pyridine in Fig. 8).*

S l i k a 9 – *Prikaz tipa Esin i Markov za utjecaj adsorpcije pirazina na ugljenoj elektrodi; pomak potrencijala, ΔE, kod četiri razne veličine promjene površinskog naboja, Δq, (temeljeno na izvedenim podacima u odnosu na potencijal od –0,08 V prema Ag/AgO), prikazane kao funkcija stupnja adsorpcije 1,4-pirazina, Γ: (■) 0,5 10⁻⁴ C m⁻²; (✳) 4 × 10⁻⁴ C m⁻²; (▲) 6 × 10⁻⁴ C m⁻² and (☆) 10 × 10⁻⁴ C m⁻². (Nema infleksija kakve su vidljive kod piridina na slici 8).*

The interfacial capacitance is given by the well known formula in electrostatics:

$$C_X = \frac{A \varepsilon \varepsilon_0}{d} \qquad (6)$$

For a surface area A (cm^2), with surfaces of the capacitor being separated by a distance d (cm) containing the interphasial dielectric of constant ε and where ε_o is the dielectric permittivity of free space (8.85×10^{-12} F m^{-1}). Equation (6) predicts values of C_x on the order of 15 to 30 μF cm^{-2}, depending on the dielectric permittivity, ε, of the interphase, taking d as 0.2 to 0.3 nm.

The important practical aspect of interfacial capacitance of electrodes is that it has very high values (as noted above), orders of magnitude greater than that of the capacitance per cm^2 of hardware capacitor devices having thin-layer material dielectrics, *e.g.*, mica, polystyrene, or even thin oxide films of *e.g.* TiO_2, Ta_2O_5, Al_2O_3, as in electrolytic capacitors. This is because, in Eq. 6, the thickness, d, of the dielectric of the double-layer is only some 0.2 – 0.3 nm. Hence, the actual interfacial double-layer capacitance that can be developed at high specific-area carbon electrodes is very high, which makes device development of electrochemical capacitors, a practically attractive proposition. Use of the capacitance of the double-layer at porous C electrodes, as a basis for charge storage, is thus the ultimate application of interfacial properties of charged interfaces studied earlier at colloids[23] and at Hg electrodes.[15,16]

It is easily seen that, for a C interface having, say, a specific double-layer capacitance of ca. 25 μF cm^{-2} at a material having say, 2000 m^{2}g^{-1} in available area for charging can hence exhibit a capacitance of $25 \times 10^{-6} \times 2000 \times 10^4$ F g^{-1}, i.e. 500 F g^{-1}! Over a 1 volt charging range of potential, this corresponds ideally to an accommodation of 500 C g^{-1}! Practically achievable charge-densities are about 50 to 30 % of that figure and, in a 2-electrode capacitor device, half again of that value,[5,14] or less, see below.

For comparison, a mercury electrode in aqueous KF or K_2SO_4 solution exhibits a specific double-layer capacitance of ca. 18 μF cm^{-2} at potentials negative to the potential of zero charge (pzc) and up to ca. 30 μF cm^{-2} at positive polarizations, depending importantly on the anion of the electrolyte.[15]

For contrast, note that the "one-electron", nickel-oxide battery cathode, has a charge accommodation of 96 500 C mol^{-1}, *i.e.* ca 1060 C g^{-1}. Thus, the practical non-Faradaic charge accommodation of the above C material is about 10 – 15 % of the Faradaic accommodation of charge, per gram, of the $Ni(OH)_2$/Ni.O.OH cathode (itself) of the Ni/Cd battery.

The perceived advantage of electrical charge storage by electrochemical capacitors is that high charge/discharge rates would be achievable owing to the absence of irreversibility effects that arise in Faradaic processes on account of chemical phase changes, e.g. with the lead/acid battery where the processes Pb → $PbSO_4$ and PbO_2 → $PbSO_4$ are coupled in discharge. However, note that recent developments envisage coupling of a capacitor electrode with a Faradaic one in an asymmetric hybrid device. In charging of double-layer capacitor electrodes, only accumulation of ionic and electronic charges across the electrode interfaces takes place. However, because high specific capacitance is only achieved by use of electrodes having large specific areas and hence an high degree of pore structure, a distributed resistance arises in the matrix and behaves like a transmission line.[12] This corresponds to a spectrum of "*RC*" time-constants so that the charging behaviour corresponds to a "power spectrum": at high frequencies or short pulse-times, the matrix remains only partially charged, but more complete charging is achieved over longer time-scales, ultimately under d.c. conditions.

Some interfaces of special materials, *e.g.* (see refs. 5 and 9) RuO_2 or conducting polymers (polyaniline, polythiophene), develop pseudocapacitance which is Faradaic in origin yet behaves like a capacitance since charge accumulation is approximately proportional to polarization voltage, so that a measurable and large specific capacitance arises, often some 10 to 50 times larger per unit area or per gram than that of double-layer capacitance for the same mass or area of the electrode material.

These situations have led to major activity over the past 15 years or so for development of electrochemical supercapacitors, though earlier embodiments date back to ca. 1970[7] and to a US patent for a primitive carbon device in 1958.[24] A recent monograph[5] by the present, senior author described the developments in this field in extensive detail, together with the fundamental science that is involved.

Although a single electrode interface behaves as a capacitance, for use in a practical device, two electrodes are required (as in a battery), one worked against the other, with different directions of polarization, + and –, on charge. This results in the device capacitance being determined by the series relationship:

$$1/C = 1/C_+ + 1/C_- \quad (7)$$

Then, for a symmetrical capacitor ($C_+ = C_-$) the net measurable device capacitance is

$$1/C = 2/C_+ \text{ or } 2/C_- \quad (8)$$

so that

$$C = C_+/2 \text{ or } C_-/2 \quad (9)$$

i.e., half the individual electrode capacitances. Also, if one electrode has an appreciably larger capacitance than the other, then it is the *smaller value* that determines the experimental capacitance.

Another practical aspect is that, since the energy-density on charge to a device voltage, ΔV, is $^1/_2\ C\ (\Delta V)^2$, once the voltage diminishes on discharge to say 50 % of its initial value, the stored energy-density has fallen to 25 % of its initial value which would correspond to 12.5 % of the initial capacitance of each electrode!

New concepts of electrochemical capacitor design envisage coupling one double-layer capacitor electrode with a Faradaically chargeable electrode such as Pb/PbO_2 or $Ni(OH)_2/Ni{\cdot}O{\cdot}OH$, referred to earlier. This has the effect of improving the energy-density since the Faradaic electrode loses much less percentage voltage on discharge than does the capacitor electrode since the latter, for fundamental reasons, has an (almost) linearly falling voltage with decline of state of discharge. The conditions for optimizing the performance of such a combination have been treated in a previous recent publication by us.[25] Such "capacitor" devices are referred to as "hybrid" or "asymmetric" capacitors; one electrode has good energy-density the other good power-density giving, overall, a net improvement in performance, *e.g.* an higher cell voltage is maintained on discharge, and Eq. 7 is no longer applicable.

Characterization of behaviour of electrochemical capacitors

Three principal experimental procedures have been employed for evaluation of the electrical performance of electrochemical capacitor electrodes and two-, or multiple-, electrode devices for charge storage and delivery; they are:

a) Cyclic voltammetry (CV) conducted at various sweep-rates. This procedure gives directly the capacitance as $C = i/v$ (Fig. 1) where i is the response current (or current-density) for an applied voltage sweep-rate of v (Vs^{-1}). This gives directly a differential capacitance, integration of which, over the time (or voltage span), gives the accepted or delivered charge. This procedure is very useful as it gives immediately a profile of capacitance as a function of potential over the scanned range (ca. 1.2 V in aqueous solutions, 3 – 3.5 V in aprotic, non-aqueous solvents) and also any *dispersion* of capacitance that can arise with increasing sweep-rate due to series e[12]) drop (equivalent series resistance, ESR) and/or to the usually significant, internal distributed resistance (*de Levie[12]*) of the electrolyte-containing porous-C matrix. The current response profiles in CV, recorded at various v values also gives a facile evaluation of the "C-rate" (in battery terminology); C/1 = rate for which all the available charge is withdrawn (or accumulated) on charging in 1 hour. Experimental CV data show that discharge/recharge rates can be very high, up to ca. 20 C (compare optimum rate of C/4 for lead/acid battery operation), a situation that arises because only electrostatic charging is involved at the double-layer and not Faradaic phase- changes (which are often slow and kinetically irreversible) that arise in battery charge/discharge processes.

b) Impedance spectroscopy, conducted over a wide range of modulation frequencies. This is an obvious procedure for evaluation of capacitance and is complementary to CV. However, due to the complexity of the equivalent-circuit for porous electrodes (Fig. 10 and *de Levie*[12]) and the possibility of some involvement of adsorption or redox pseudo-capacitance, analysis of impedance spectroscopy can be quite complex but, when conducted carefully, is valuable for device-performance evaluation.

c) Also complementary to CV, is the classical procedure of constant-current charging or discharging, usually conducted at various rates (current-densities). This gives the integral charging behaviour and is useful for identification of series $I\,R$-drop values and as a procedure for evaluation of energy-density (ED), and power-density (PD) data giving rise to Ragone Plots for ED vs. PD. The latter types of plots have major value in comparative performance evaluations for various supercapacitor devices.

d) Experiments of a different kind for device applications are i) cycle-life tests at various temperatures (practical cycle-lives required are minimally several thousands or, ideally, tens of thousands) and ii) evaluation of open-circuit self-discharge rates which are often greater than for battery systems such as Li primary cells or Pb/acid batteries. From the functionality of the dependences of electrode-potential on time on open-circuit self-discharge (*e.g.* on log t, exp t or $t^{1/2}$), the mechanism of the self-discharge process can be elucidated as treated in ref. 26.

Equivalent-circuits for electrical behaviour of electrochemical capacitor electrodes

The kinetic interpretation of charging processes at capacitative electrode interfaces, especially when such surfaces are distributed in a porous-electrode matrix, has to be based on an *equivalent-circuit model*. This is especially the case when experimental evaluation is made by CV and/or impedance spectroscopy, and rate effects are of importance in device behaviour.

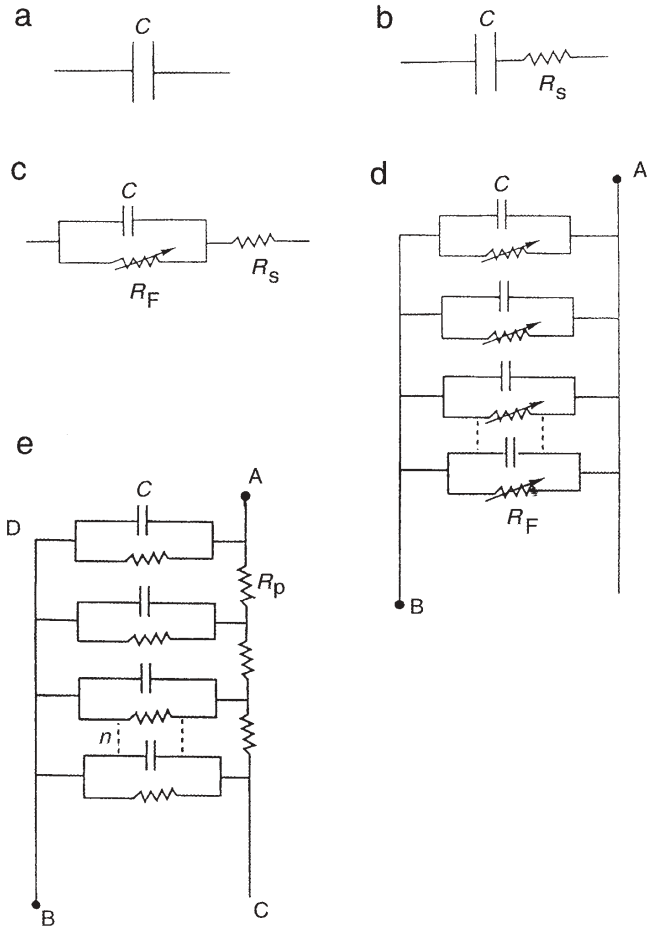

F i g . 10 – *Hierarchy of equivalent circuits of increasing complexity for capacitors and electrochemical capacitors, through to the* de Levie[9,10] *transmission line model: (**a**) simple capacitor; (**b**) capacitor with equivalent or real series resistance; (**c**) capacitor with series resistance and potential-dependent faradaic leakage resistance, R_f; (**d**) parallel combination of n C and R_f leakage elements. Overall "RC" constant is R_f/n n C = R C for the single element; (**e**)* (de Levie *transmission line model) parallel C, R_f elements, and series R_p related to transmission line, constant phase element but with R_f leakage pathways.*

S l i k a 10 – *Ekvivalentni krugovi rastuće složenosti za klasične i elektrokemijske kondenzatore sve do de Leviejevih modela prijenosnih linija: (**a**) jednostavni kondenzator, (**b**) kondenzator s ekvivalentom stvarnog otpora u seriji, (**c**) kondenzator s otporom u seriji i potencijalom ovisnim o faradejskom otporu samopražnjenja, R_f (d) paralelna $R_f/n \times n\,C = R/C$ za jedan element; (**e**) de Leviejev model prijenosnih linija), paralelni elementi C i R_f te serija R_p povezana s prijenosnom linijom, element konstantne faze, ali s R_f putem samopražnjenja.*

It is convenient to consider the situation in terms of an hierarchy of equivalent circuits that represent, in increasing complexity, the behaviour of electrode interfaces beginning with the simplest case, that of a double-layer capacitance at a plane metal interface without impediment to charging by any series resistance, then with capacitance in series with a solution resistance and on to a series/parallel combination of resistance and capacitance elements that represent the dynamic behaviour of a porous electrode matrix according to the model and treatment of *de Levie*[12] and to the direct hardware *C R* circuit-modeling conducted experimentally by *Pell* et al.[27]

The hierarchy of such model circuits is illustrated in Fig. 10 where circuit (e) represents that of a porous electrode. Circuits involving simply a series or parallel combination of *C* and *R* elements exhibit a relaxation time-constant of magnitude *R C* with frequency-dependent impedance; the parallel combination exhibits leakage, and is thus a model for open-circuit self-discharge of capacitive electrodes. Circuit (e) involves a matrix of series/parallel combinations of *R* and *C* elements representing the impedance to signals experienced down a pore of a porous electrochemical capacitor electrode. The electrical behaviour on charging or on alternating voltage (impedance evaluation) modulation is that of a complex combination of *R C* time-constants giving rise to impedance behaviour corresponding to that of a transmission line.[12] Practically, this means that such an electrode exhibits a *power spectrum*. Elements of pores near matrix interfaces with the electrolyte solute can be charged or discharged at high rates (small *R C* time-constants) while inner elements suffer a dispersion of charging rates to lower values due to the larger time-constants that apply on account of the progressive increase of resistance down pores in the matrix (Fig. 10e). Under dc charging, however, all of the internal capacitance is eventually charged (or vice-versa on discharging).

De Levie[12] explains this situation in terms of a frequency (or rise-time) – dependent signal penetration effect down pores, i.e. at high frequencies, only a fraction of pore-lengths are charged or discharged while at low frequencies, charging penetrates deeper into the pore structure. This concept of signal attenuation is fundamental to understanding the difference of the dynamics of charging a porous electrode structure (circuit e) from that for the elementary circuits (a or b) in Fig. 10. It is also of major practical significance in understanding limitations of power performance of capacitor electrodes in supercapacitor devices designed for various purposes in engineering applications and characterizing performance in terms of effective time constants and overall ohmic impedance: values down to the milliohm range are now commonly achieved. However, it is important to recognize that, unlike the situation for ideal batteries, achievable energy-, and power-densities are, for fundamental reasons, dependent on state-of-charge. This is, of course, because the voltage, *V* across a capacitor is directly dependent on the charge-density, q, residing on its plates: $V = q/C$.

The consequences of this relation are manifested in all aspects of comparisons between capacitor devices and batteries except where the latter exhibit pseudocapacitance,[5] [see chapter 10],[5] e.g. as in some cases of systems involving intercalation of Li^+ ions into oxide or sulphide host matrices where electrode-potentials are commonly dependent on state of charge giving rise to a potential-dependent, differential pseudocapacitance (see chapter 2, p. 26 in ref. 5).

Relation between energy-density and power-density: Ragone plots

Energy-utilizing systems can be operated at various rates corresponding to development of various power levels. This applies as much to electrochemical energy/power sources as to mechanical systems such as internal combustion

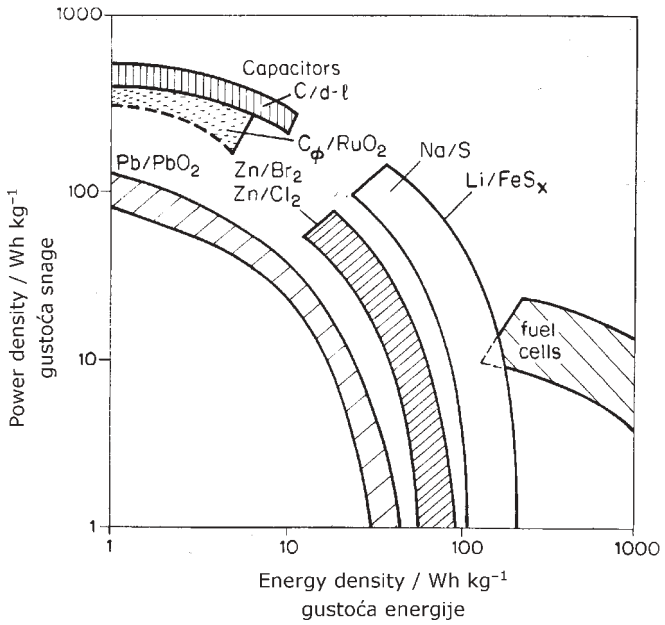

F i g . 11 – *Examples of Ragone plots of energy-density versus power-density for some battery and capacitor systems*

S l i k a 11 – *Primjeri Ragoneovih prikaza gustoće energije kao funkcije gustoće snage za neke baterijske i kondenzatorske sustave*

engines, turbines etc. However, for quite general thermodynamic reasons, irreversible dissipation of energy (energy losses) always accompany operations at higher power levels.

In the case of batteries and electrochemical capacitors, the energy-density (ED) is measured in watt-hours and the corresponding power (PD) in watts. Energy-densities are measured by charge multiplied by voltage at which the former are stored and available while power-densities are determined by the currents drawn multiplied by that voltage. Ohmic (resistive, *R*) energy losses arise at rates $i^2 R$ leading to power losses by diminution of operating voltage on account of $i R$-potential losses or by kinetic overvoltage, η, losses, giving rise to $i\eta$ rates of energy loss. The former determine the energy losses that arise with increasing power drain in the case of electrochemical capacitors while both effects operate in the case of battery discharge or recharge; see Figs. 11, 12, 13, and below.

Relations between ED and PD, referred to as Ragone plots (*D. Ragone*),[28] are of central importance as a basis for specifying performance parameters for batteries and capacitors. Such plots are conveniently derived by recording charging curves at various, different but constant rates, i.e. current-densities or power levels, and deriving the usual rate-dependent stored energies, the latter being given, for capacitors, by the equation

$$ED = {}^1/_2\, CV^2 = {}^1/_2\, q\, V \qquad (10)$$

where V is the voltage or potential at V which charge, q, is accumulated. The rate-dependence of ED arises because the voltage, V, drops when charging or discharging is conducted at increasing rates due to the factors identified above. However, as noted earlier, an additional factor of importance in making Ragone plots for capacitors is that the voltage on charge or discharge depends directly on the *state-of-charge* so that ED and PD decline for fundamental reasons with decreasing state-of-charge. (Similar effects can arise to some extent with batteries but for more trivial reasons).

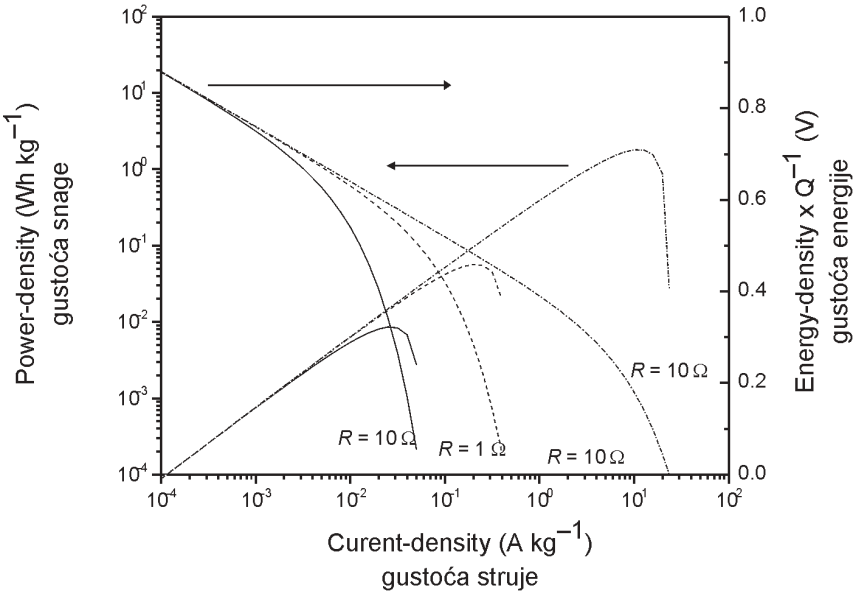

F i g . 12 – *The effect of ohmic polarization on PD and reduced ED as a function of i for a battery characterized by $\Delta V_{rev} = 1$ V, $i_0 = 10^{-5}$ A kg^{-1}, b = 0.120 V, and a = 0.60 V*

S l i k a 12 – *Utjecaj omske polarizacije na gustoću snage i smanjenu gustoću energije kao funkcija struje za bateriju sa $\Delta V_{rev} = 1$ V, $i_0 = 10^{-5}$ A/kg, b = 0,120 V i a = 0,60 V*

Data for ED and PD are usually plotted against each other on double logarithmic scales in the Ragone relations in order to cover a wide range of discharge or recharge rates. An example is shown in Fig. 11.

Pell and *Conway*[29] made numerical calculations of the factors determining the forms of Ragone plots for battery and capacitor systems. Examples are shown and discussed as follows. They showed how Ragone plots can be constructed by separate calculations of PD and of ED versus current-density for various, arbitrarily selected values of ohmic resistance, R, (in the case of capacitor behaviour) or of the Tafel-slope (b) polarization parameter for a given value of R (taken nominally as 1 ohm). In the latter case for battery evaluation, both the kinetic polarization η (determined by the slope parameter, (b) and the exchange current-density, i_o, for the battery electrode process determine the form of the Ragone plot. For an actual two-electrode cell, account has to be taken

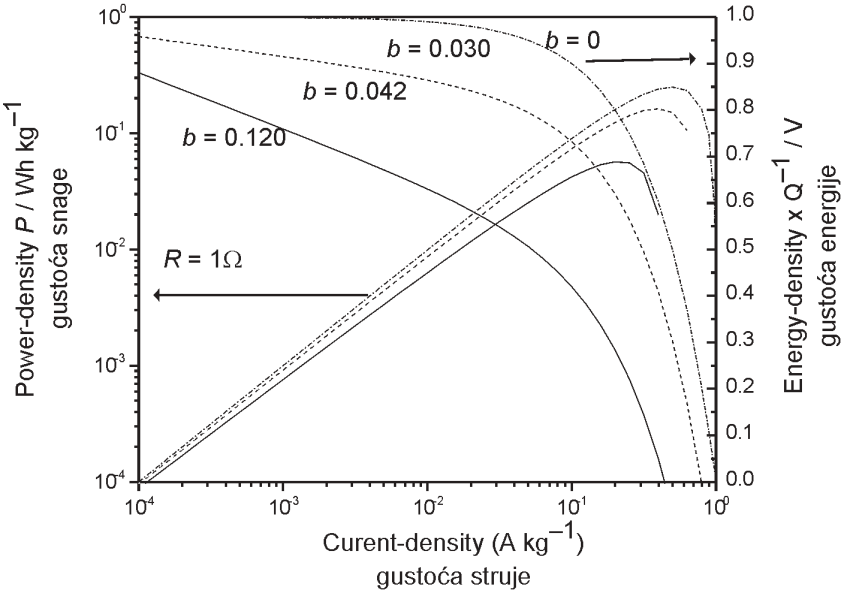

F i g . 13 – *The effect of Tafel polarization on PD and reduced ED as a function of i for a battery characterized by* $\Delta V_{rev} = 1$ *V,* $i_0 = 10^{-5}$ *A kg*$^{-1}$*, and* $R = 1\ \Omega$

S l i k a 13 – *Utjecaj Tafelove polarizacije na gustoću snage i smanjenu gustoću energije kao funkcija struje za bateriju sa* $\Delta V_{rev} = 1$ *V,* $i_0 = 10^{-5}$ *A kg*$^{-1}$ *i* $R = 1\ \Omega$

of the polarization behavior of *each* of the two complementary electrodes. Usually, the Ragone behavior of a battery cell is determined more by one electrode (the more polarizable one) than the other, together, importantly, by the specific conductivity (*i R*-effect) of the cell's electrolyte and thence also by the operating temperature.

From the separate evaluation (Fig. 12 or Fig. 13) of PD and ED vs. operating current-density, the required Ragone plots can be obtained by plotting PD vs. the corresponding ED as illustrated in Fig. 14 for the case of electrochemical capacitor electrodes. Note that the Ragone plots for capacitors depend on state-of-charge[29] (for the reasons cited earlier). The ohmic and kinetic polarization effects that lead to diminution of ED with increasing operating PD in the Ragone plots are also the factors that cause distortion of cyclic voltammograms (Fig. 1) and DC charging curves conducted at progressively increased rates (larger sweep-rates or increasing constant-current charging). Computer modeling calculations in ref.[30] show how the distortion effects can be quantitatively normalized out of the experimental behaviour by plotting the response variable, *i*/*v*, versus *i R*-corrected values of the experimentally applied (measured) potential, V_m, thus providing a corrected ("inner") local working electrode polarization potential scale, V_e, for CVs and charging curves.

Comparative capacitance behaviour of various types of porous carbon

We have indicated, in section 1, that a variety of porous C materials are now available for development of supercapacitors; some are derived as charcoals by pyrolysis of natural materials and others by controlled pyrolysis of organic polymers. New materials are in the form of aerogels or C "nanotubes", based on fullerene structures. Recent information on such electrodes can be found in the various printed proceedings contributions in the series of Seminars on Double-Layer Capacitors and Hybrid Energy Storage Devices.[31] Most porous C materials for high specific-area electrodes require special conditioning treatments at elevated temperature in N_2 or stream in order to open up nano-scale porosity and corresponding enhanced specific real area. Primary comparative characterization of capacitative behaviour is conveniently achieved by means of cyclic voltammograms (CV), as exemplified in Fig.1 for our electrode material which gives CVs, closely approaching the ideal rectangular form expected for a pure capacitance, independent of potential, as also found for RuO_2.[11] However, depending on provenance of the C and its conditioning pretreatment, a variety of forms of CVs can arise as illustrated in chapter 6.1,[8] some (e.g. graphitic materials) not well ap-

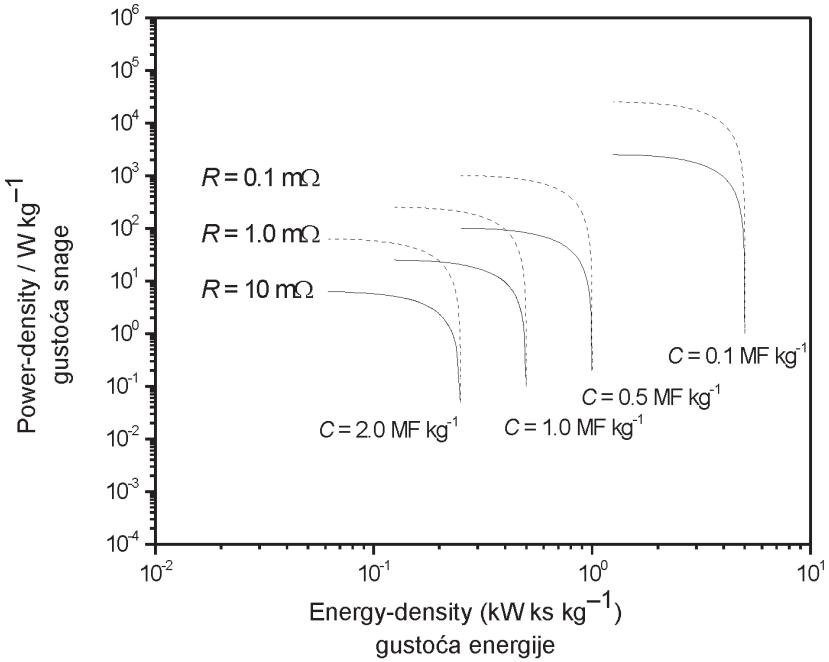

F i g . 14 – *Calculated Ragone plots for fully charged capacitors having constant Q = 1 MC kg*$^{-1}$*, variable nominal C (= 2.0, 1.0, 0.5 and 0.1 MF kg*$^{-1}$*) values*

S l i k a 14 – *Proračunati Ragoneov prikaz za potpuno nabijen kondenzator koji ima konstantni naboj Q = 1 MC kg*$^{-1}$*, s raznim nominalnim vrijednostima kapaciteta C (= 2,0, 1,0, 0,5 i 0,1 MF kg*$^{-1}$*)*

proximating to the almost ideal capacitative behaviour found with the C-cloth material examined in the present work.

With regard to comparative adsorptive behaviours of various carbons (ref.1) in comparison with our own (Figs. 2 to 9), little further information is available and none based on our quantitative, *in situ*, spectroscopic methodology.

References
Literatura

1. *K. Rajeskwar, J. Ibanez,* Environmental Electrochemistry, Academic Press, New York, 1997.
2. *B. E. Conway, E. Ayranci, H. Al-Maznai,* Electrochim. Acta **47** (2001) 705.
3. *H. Wroblowa,* J. Electroanal. Chem. **49** (1974) 355.
4. *J. Niu, B. E. Conway,* J. Electroanal. Chem. **536** (2002) 83.
5. *B. E. Conway,* Electrochemical Supercapacitors; Scientific Principles and Technological Applications, Kluwer-Plenum Publ. Co., New York, 1999.
6. *B. E. Conway,* J. Electrochem. Soc. **138** (1991) 1539.
7. *D. L Boos,* US patent 3,536, 963 to Standard Oil Co. 1970.
8. *K. Kinoshita,* Carbon (chapter 3), Wiley-Interscience New York, 1988.
9. *B. E. Conway, J. Wojtowicz, V. Birss,* J. Power Sources, **66** (1997) 1.
10. *B. E. Conway, E. Gileadi,* Trans. Faraday Soc. **58** (1962) 2493.
11. *G. Buzzanca, S. Trasatti,* J. Electroanal. Chem. **23** (1971) App. 1.
12. *R. de Levie,* Electrochim. Acta **8** (1963) 751.
13. *H. Keiser, K. D. Beccu, M. A. Gutjahr,* Electrochim. Acta **21** (1976) 539.
14. *J. Miller* in Proc. 5th Intl. Seminar on Electrochemical Double-layer Capacitors and Similar Devices, Deerfield Beach, FL. 1995.
15. *D. C. Grahame,* Chem. Rev. **41** (1947) 441.
16. *J. A. V. Butler,* Proc. Roy. Soc., London, **A122** (1929) 399.
17. *J. Niu, B. E. Conway,* J. Electroanal. Chem. **521** (2002) 16.
18. *J. Niu, B. E. Conway,* J. Electroanal. Chem. **529** (2002) 84.
19. *J. O'M. Bockris, M. A. V. Devanathan, K. Müller,* Proc. Roy. Soc., London, **A274** (1963) 55.
20. *R. Parsons,* J. Electroanal. Chem. **59** (1975) 229.
21. *S. Marshall, B. E. Conway,* J. Electroanal. Chem. **137** (1992) p. 19, 45 and 67.
22. *A. Ben Naim,* Hydrophobic Interactions, Plenum Publ. Co., New York, 1980.
23. E.g. see chapter V in *A. W. Adamson,* Physical Chemistry of Surfaces (4th edn.), John Wiley and Sons, New York, 1982.
24. *H. L Becker, V. Ferry,* 2,800, 616 (1957) to General Electric Co.
25. *W. G. Pell, B. E. Conway,* J. Power Sources **136** (2004) 334.
26. *W. G. Pell, T. C. Liu, B. E. Conway,* J. Power Sources **65** (1997) 53.
27. *W. G. Pell, B. E. Conway, W. A. Adams, J. de Oliviera,* J. Power Sources **80** (1999) 134.
28. *D. Ragone* in Proc. Automotive Engineers Conference on Review of Battery Systems, Soc. Automotive Engineers, Warrendale, PA., 1968; for further details, see chapter 15 in ref. 5 above.
29. *W. G. Pell, B. E. Conway,* J. Power Sources **63** (1996) 255.
30. *W. G. Pell, B. E. Conway,* J. Power Sources **96** (2001) 57.
31. Various printed papers in Proceedings of the 14th and 13th International Seminars on Double-Layer Capacitors and Hybrid Energy Storage Devices, Deerfield Beach, December 2004 and 2003, Ed. *N. Marincic,* Redox Engineering LLC, 215 Dolphin Cove Court, Bonita Springs, FL 34134. See also Proceedings of earlier Seminars organized by *N. Marinčić* and *S. Wolsky,* Florida Educational Seminars Inc., 1900 Glades Road, Suite 348, Boca Raton, FL 33431.

SAŽETAK

Elektrokemija na ugljenim elektrodama visoke specifične površine: primjena u adsorptivnom pročišćavanju voda i u pohranjivanju naboja u superkondenzatorima

B. E. Conway, J. Niu i W. G. Pell

Razne vrste elementarnog ugljika (C) upotrebljavaju se naveliko u elektrokemiji kao prah velike specifične površine, pusta, tkanina, aerogel ili fulerenske cjevčice. Ovaj rad je pregled i rasprava o novijim radovima u kojima je primijenjeno ugljeno platno velike specifične površine (do 2500 m^2g^{-1}) kao elektrodni materijal za adsorpcijsko odstranjivanje organskih primjesa modelnih otopina otpadnih voda i za pohranjivanje i dobavu električnog naboja u elektrokemijskim kondenzatorima (takozvanim superkondenzatorima). Ta dva oblika ponašanja C-elektroda proizlaze iz svojstava međufaznog dvosloja u kojima se odvija i elektrosorpcija i odlaganje električnog naboja, uz vidljiv utjecaj druge na prvu od tih pojava.

Takvi ugljeni materijali pokazuju veliku učinkovitost u adsorptivnom odvajanju jednostavnih aromatičnih heterocikličkih spojeva, dok primjena napona ili struje, ili primjena raznih otapala izaziva velike promjene u stupnju adsorpcije. Usporedo s adsorpcijom isto ugljeno platno velike specifične površine pokazuje veliku gustoću elektrokemijskog kapaciteta (250–500 Fg^{-1}), što omogućuje primjenu ovog materijala kao elektroda u superkondenzatorima. Navedeni su primjeri ispitivanja dobave i pohrane električnog naboja, posebno uz visoke struje, koji dovode do privlačnih vrijednosti gustoće energije i s gustoćom snage znatno višom od one u baterijama.

Chemistry Department University of Ottawa
10 Marie Currie Street, Ottawa, ON. KIN 6N5, Canada

Prispjelo 16. kolovoza 2004.
Prihvaćeno 11. siječnja 2005.